J|A|C|S
ARTICLES
Published on Web 02/22/2002

Mechanism of OH Formation from Ozonolysis of Isoprene: A Quantum-Chemical Study

Dan Zhang and Renyi Zhang*

Contribution from the Department of Atmospheric Sciences, Texas A&M University, College Station, Texas 77843

Received June 21, 2001. Revised Manuscript Received October 16, 2001

Abstract: The formation and unimolecular reactions of primary ozonides and carbonyl oxides arising from the O_3-initiated reactions of isoprene have been investigated using density functional theory and ab initio molecular orbital calculations. The activation energies of O_3 cycloaddition to the two double bonds of isoprene are found to be comparable (3.3−3.4 kcal mol^{-1}), implying that the initial two O_3 addition pathways are nearly equally accessible. The reaction energies of O_3 addition to isoprene are between −47 and −48 kcal mol^{-1}. Cleavage of primary ozonides to form carbonyl oxides occurs with a barrier of 11−16 kcal mol^{-1} above the ground state of the primary ozonide, and the decomposition energies range from −5 to −13 kcal mol^{-1}. OH formation is shown to occur primarily via decomposition of the carbonyl oxides with the syn-positioned methyl (alkyl) group, which is more favorable than isomerization to form dioxirane (by 1.1−3.3 kcal mol^{-1}). Using the transition-state theory and master equation formalism, we determine an OH yield of 0.25 from prompt and thermal decomposition of the carbonyl oxides.

Introduction

Atmospheric photochemical oxidation of volatile organic compounds (VOCs) is initiated by a variety of oxidant species, including OH, O_3, NO_3, and halogen radicals. Among the various oxidants, hydroxyl radicals play the most central role in determining the oxidation power of the atmosphere.[1,2] OH radicals react with VOCs to produce organic peroxy radicals which facilitate cycling of NO to NO_2, a critical step in tropospheric ozone formation. A substantial portion of the VOCs, particularly alkenes, may also be degraded by reaction with ozone. There exists increasing evidence that OH radicals are generated during the course of this ozonolysis.[3] The ozonolysis of olefins has long been considered as a fundamental and intriguing chemical problem, from both the experimental and theoretical points of view. Elucidation of the underlying reaction mechanisms, however, has represented a major challenge due to the inherent complexity.

Isoprene is one of the most abundant hydrocarbons naturally emitted by the terrestrial biosphere;[4] ozonolysis of isoprene provides an important source of nighttime OH radicals on the regional scale.[5] Since the O_3–isoprene reactions are linked to several key tropospheric species (O_3, isoprene, and OH) and could also play a role in aerosol formation (oxidation of SO_2 by carbonyl oxides),[6] the atmospheric effects of the isoprene ozonolysis are potentially far-reaching. The ozonolysis of isoprene proceeds through a complex series of reactions and intermediates. The initial reaction between isoprene and O_3 (R1) occurs by cycloaddition of O_3 to the >C═C< double bonds, forming the primary ozonide, a five-membered ring from O_3 addition to either of the isoprene's double bonds. The addition is thermally allowed in accordance with the Woodward−Hoffmann symmetry roles;[7] the available reaction energy is retained as the internal energy of the product, resulting in formation of the vibrationally excited ozonide. The excited ozonide subsequently undergoes unimolecular decomposition (R2) to yield a chemically activated biradical, known as the carbonyl oxide or Criegee intermediate (CI), and an aldehyde. A large fraction of the carbonyl oxide will have ample internal energy, rendering it susceptible to unimolecular reactions or stabilization. There are two primary reaction pathways for the carbonyl oxide, ring closure to dioxirane (R3a) or H-migration to form a hydroperoxide intermediate (R3b). The hydroperoxide subsequently decomposes to form OH and RCO radicals (R3c). Schemes 1 and 2 illustrate the mechanistic diagrams for the formation and unimolecular reactions of the primary ozonides and carbonyl oxides, respectively.

In addition, there may exist other possible OH formation mechanisms. One such pathway involves nonconcerted decomposition of the primary ozonide by a stepwise mechanism.[8] The stepwise path begins with cleavage of the O−O bond, leading to a biradical, which in turn decomposes into an unstable hydroperoxide. Recent theoretical calculations, however, differ

* To whom correspondence should be addressed.

(1) Seinfeld, J. H.; Pandis, S. N. *Atmospheric Chemistry and Physics: From Air Pollution to Climate Change*; John Wiley & Sons: New York, 1997.
(2) Thomson, A. M. *Science* **1988**, *256*, 1157.
(3) Atkinson, R. *J. Phys. Chem. Ref. Data* **1997**, *26*, 215.
(4) Trainer, M.; et al. *Nature* **1987**, *329*, 705.
(5) Biesenthal, T. A.; Bottenheim, J. W.; Shepson, P. B.; Brickell, P. C. *J. Geophys. Res.* **1998**, *103*, 25487.
(6) Hatakeyama, S.; Kobayashi, H.; Lin, Z. Y.; Tagaki, H.; Akimoto, H. *J. Phys. Chem.* **1986**, *90*, 4131.
(7) Bailey, P. S. *Ozonation in Organic Chemistry*; Academic Press: New York, 1978; Vol. 1; 1982; Vol. 2. (b) Woodward, R. B.; Hoffman, R. *The Conservation of Orbital Symmetry*; Verlag Chemie GmSH: Weinheim, Germany, 1971.
(8) Herron, J. T.; Huie, R. E. *J. Am. Chem. Soc.* **1977**, *99*, 5430.

10.1021/ja011518l CCC: $22.00 **© 2002 American Chemical Society**

Scheme 1

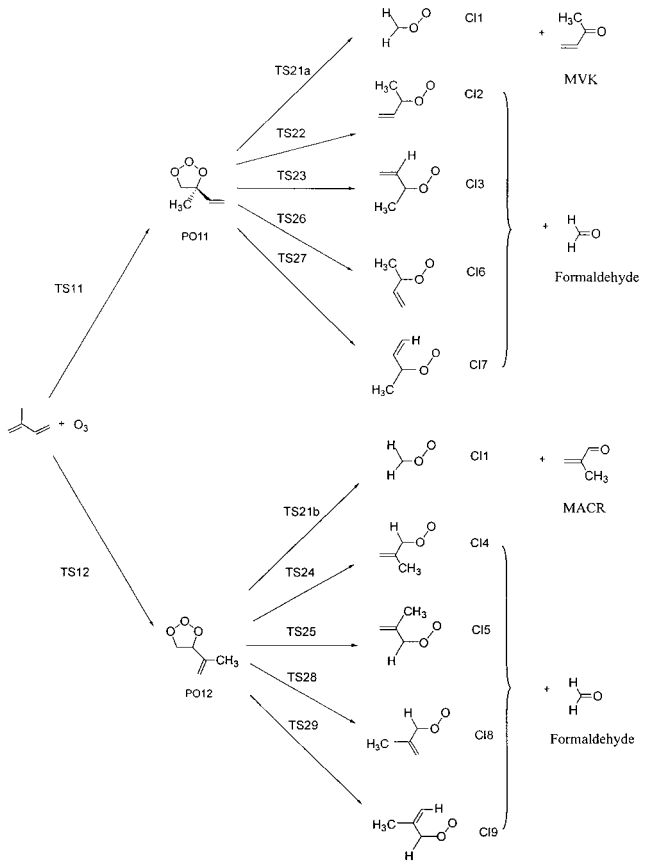

Scheme 2

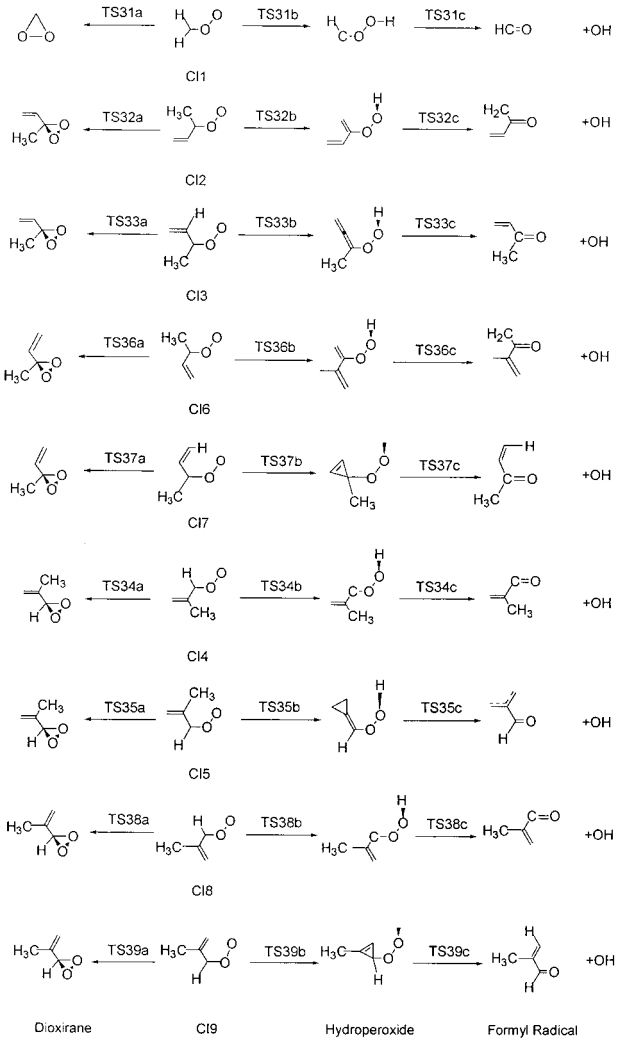

on the relative activation barriers of the nonconcerted steps and on the importance of this pathway.[9,10] Also, it has been proposed that decomposition of dioxirane may lead to formation of vibrationally excited organic acids, which may also dissociate to form OH.[11]

Current knowledge of the O_3–isoprene reaction system is very limited. Except for the initial step, there are no experimental or theoretical kinetic results on the subsequent reactions.[3] Efforts to elucidate the reaction mechanism are hindered due to the uncertain fate of the reactive intermediates, which have multiple accessible reaction pathways. Since most of the intermediates have very short lifetimes, experimental detection of these species is extremely difficult. Numerous experimental studies have been carried out to measure the OH formation yield from ozonolysis of isoprene.[12−14] In the majority of the laboratory experiments, OH scavengers or tracers were used to deduce the OH formation yield.[12,13] Alternatively, direct OH detection from the O_3–isoprene reactions has been reported using the laser-induced fluorescence (LIF) technique.[14] The available results of the OH formation yield from the various experimental studies are rather conflicting, with values in the range of 0.19−0.53 near atmospheric pressure.[13] Also, competition between collisional stabilization and unimolecular reactions of the reaction intermediates may result in pressure- and time-dependent OH yields, further complicating interpretation of the laboratory data.[15]

A previous theoretical study has investigated the importance of carbonyl oxides on OH formation in the O_3–isoprene reactions.[16] Gutbrod et al. suggested the formation of various syn and anti stereoisomers of the carbonyl oxides and reported their structures and energies at the B3LYP/6-31G(d,p) level of theory;[16] their calculations indicated that OH formation depends on a syn-positioned methyl (alkyl) group and the interaction with the terminal O atom of a carbonyl oxide. From the computation point of view, carbonyl oxides have also received considerable attention over the past three decades. Because of their weak stability, theoretical calculations are useful in determining the geometric and electronic structures of this class of compounds. A large number of theoretical studies of the electronic nature and structures of the carbonyl oxides have been reported.[9,10,14,16−21] However, formation and decomposition of the

(9) Fenske, J. D.; Hasson, A. S.; Paulson, S. E.; Kuwata, K. T.; Ho, A.; Houk, K. N. *J. Phys. Chem.* **2000**, *104*, 7821.
(10) Anglada, J. M.; Crehuet, R.; Bofill, J. M. *Chem.—Eur. J.* **1999**, *5*, 1809.
(11) Harding, L. B.; Goddard, W. A. I. *J. Am. Chem. Soc.* **1978**, *100*, 7180.
(12) Atkinson, R.; Aschmann, S. M.; Arey, J.; Shorees, B. *J. Geophys. Res.* **1992**, *97*, 6065. (b) Aschmann, S. M.; Arey, J.; Atkinson, R. *Atmos. Environ.* **1996**, *30*, 2939. (c) Gutbrod, R.; Meyer, S.; Rahman, M. M.; Schindler, R. N. *Int. J. Chem. Kinet.* **1997**, *29*, 717. (d) Paulson, S. E.; Chung, M.; Sen, A. D.; Orzechowska, G. *J. Geophys. Res.* **1998**, *103*, 25333. (e) Neeb, P.; Moortgat, G. K. *J. Phys. Chem.* **1999**, *103*, 9003.
(13) Lewin, A. G.; Johnson, D.; Price, D. W.: Marston, G. *Phys. Chem. Chem. Phys.* **2001**, *3*, 1253.
(14) Donahue, N. M.; Kroll, J. H.; Anderson, J. G.; Demerjian, K. L. *Geophys. Res. Lett.* **1998**, *25*, 59.
(15) Kroll, J. H.; Clarke, J. S.; Donahue, N. M.; Anderson, J. G.; Demerjian, K. L. *J. Phys. Chem.* **2001**, *105*, 1554.
(16) Gutbrod, R.; Kraka, E.; Schindler, R. N.; Cremer, D. *J. Am. Chem. Soc.* **1997**, *119*, 7330.
(17) Olzmann, M.; Kraka, E.; Cremer, D.; Gutbrod, R.; Andersson, S. *J. Phys. Chem.* **1997**, *101*, 9421.

primary ozonides arising from the O_3–isoprene reaction have not been previously investigated. Furthermore, accurate prediction of the OH formation yield requires precise description of the energetics of the O_3–isoprene reactions, which is largely dependent on the level of the quantum-chemical theory employed.[17,18,21]

This work investigates the formation and unimolecular reactions of the intermediate species arising from the O_3–isoprene reactions, in an attempt to elucidate the mechanism responsible for OH formation. The study includes the formation of the primary ozonides, cleavage of the primary ozonides to form the carbonyl oxides, and unimolecular reactions of the carbonyl oxides. Density functional theory (DFT) and ab initio methods are employed to obtain the geometries and energetics of the primary ozonides and carbonyl oxides. The transition states of formation and unimolecular reactions of these intermediates are located to identify the likely reaction pathways leading to OH formation. Effects of electron correlation and basis set on the calculated reaction and activation energies of the O_3–isoprene reactions are evaluated. A computationally efficient method for determination of the energetics of the O_3–isoprene reactions is discussed. This study presents theoretical investigation of the O_3–isoprene reactions using consistently high-level quantum chemical theory, extending from the reactants to products. In addition, we calculate the OH formation yield using the transition-state theory and master equation formalism.

Theoretical Method

The theoretical computations were performed on an SGI Origin 2000 supercomputer using the Gaussian 98 software package.[22] Geometry optimization of all reactants, intermediates, transition states, and products was executed using Becke's three-parameter hybrid method employing the LYP correction function (B3LYP) in conjunction with the split valence polarized basis set 6-31G(d,p). The DFT structures were then employed in single-point energy calculations using frozen core second-order Møller−Plesset perturbation theory (MP2) and coupled-cluster theory with single and double excitations including perturbative corrections for the triple excitations (CCSD(T)) with various basis sets. Harmonic vibrational frequency calculations were made using B3LYP/6-31G(d,p).

In the case of the ozonolysis of ethene, previous studies have evaluated various quantum-chemical approaches to identify a reliable yet economic method that provides a reasonable description of the ozonolysis reaction.[18,21,23,24] For example, an earlier study found that the inclusion of polarization functions in the basis set is important to obtain accurate energetics of the primary ozonide.[24] Other studies demonstrated that the inclusion of electron correction effects in the quantum-chemical method is essential for a reliable description of the electronic nature of the carbonyl oxides.[18,21,23] Several recent investigations revealed that an accurate description of the O_3–ethene reactions was obtained at the CCSD(T) level using a basis set of 6-311G(d,p), while other methods, which cover less correlation effects, failed to provide a consistent description of all reaction steps.[23] However, the CCSD(T)/6-311G(d,p) calculations are rather expensive when the O_3–isoprene reactions are investigated. We have recently evaluated the level of ab initio theory that applies to complex organic intermediates, on the basis of computational efficiency and accuracy.[25] We found that better convergence behavior and considerably higher computational efficiency were achieved using the density functional theory as the method of geometry and frequency calculations. Beyond the split valence polarized level of description there was little improvement in the molecular geometry when the size of the basis set was further increased (i.e., triple split, diffuse functions, expansion of the polarization portion of the basis sets, etc.). In addition, our studies for the analogous reactions of OH, Cl, or NO_3 addition to isoprene indicated that the calculated energetics were very sensitive to effects of basis set and electron correlation.[25,26]

For the intermediates arising from the O_3–isoprene reactions, single-point energy calculations at the CCSD(T) level of theory using a larger basis set (e.g., 6-311++G(d,p)) are extremely computationally demanding. We have corrected basis set effects on the calculated energetics for the O_3–isoprene reactions using an approach that has been recently developed and employed to investigate the energetics for the OH addition reaction to isoprene.[25] The procedure involved determination of a correction factor associated with basis set effects at the MP2 level and subsequent correction to the energy calculated at a higher level of electron correlation with a moderate size basis set. The basis set effects on the energies were evaluated at the MP2 level. A correction factor (CF) was determined from the energy difference between the MP2/6-31G(d) and MP2/6-311++G(d,p) levels. The values of calculated energies at the CCSD(T)/6-31G(d) level were then corrected by the MP2 level correction factors, corresponding to the CCSD(T)/6-31G(d) + CF method. In this work, we have carried out additional calculations using CCSD(T)/6-311G(d,p) to verify the energetics obtained by the basis set correction approach.

Results and Discussion

Primary Ozonides. Ozone addition occurs in a concerted fashion at the two double bonds of isoprene, i.e., the methyl-substituted double bond (C1−C2) or the unsubstituted double bond (C3−C4), leading to the formation of two distinct structural primary ozonides (**PO11** and **PO12**). For each primary ozonide, we performed calculations to locate the lowest energy conformation. The lowest energy conformations of the primary ozonides are illustrated in Figure 1. The evaluation of the vibrational frequencies confirmed that the geometries reported here represent minima on the potential energy surfaces.

For O_3 addition to isoprene, maximal overlay between the π HOMO orbital of isoprene and the π^* LUMO orbital of ozone is achieved by a parallel plane approach to the two molecules. It requires an oxygen envelope conformation for the primary ozonides. It has been suggested that conformations of five-membered ozonides are preferentially described by the two ring puckering coordinates: a puckering amplitude q representing the degree of nonplanarity and a pseudorotation phase angle ϕ defining the mode of puckering.[27] ϕ values of 0 and 180°

(18) Cremer, D.; Kraka, E.; Szalay, P. G. *Chem. Phys. Lett.* **1998**, *292*, 97.
(19) Fenske, J. D.; Kuwata, K. T.; Houk, K. N.; Paulson, S. E. *J. Phys. Chem.* **2000**, *104*, 7246. (b) Fenske, J. D.; Hasson, A. S.; Ho, A.; Paulson, S. E. *J. Phys. Chem.* **2000**, *104*, 7246.
(20) Kroll, J. H.; Sahay, S. R.; Anderson, J. G.; Demerjian, K. L. Donahue, N. M. *J. Phys. Chem.* **2001**, *105*, 4446.
(21) Aplincourt, P.; Ruiz-Lopez, M. F. *J. Am. Chem. Soc.* **2000**, *122*, 8990.
(22) Gaussian 98, revision D.3: Frisch, M. J.; Trucks, G. W.; Schlegel, H. B.; Gill, P. M. W.; Johnson, B. G.; Robb, M. A.; Cheeseman, J. R.; Keith, T.; Petersson, G. A.; Montgomery, J. A.; Raghavachari, K.; Al-Laham, M. A.; Zakrzewski, V. G.; Ortiz, J. V.; Foresman, J. B.; Cioslowski, J.; Stefanov, B. B.; Nanayakkara, A.; Challacombe, M.; Peng, C. Y.; Ayala, P. Y.; Chen, W.; Wong, M. W.; Andres, J. L.; Replogle, E. S.; Gomperts, R.; Martin, R. L.; Fox, D. J.; Binkley, J. S.; Defrees, D. J.; Baker, J.; Stewart, J. P.; Head-Gordon, M.; Gonzalez, C.; Pople, J. A., Gaussian, Inc., Pittsburgh, PA, 1998.
(23) Cremer, D.; Kraka, E.; McKee, M.; Radhakrishnan, T. P. *Chem. Phys. Lett.* **1991**, *187*, 491. (b) Cremer, D.; Gauss, J.; Kraka, E.; Stanton, J. F.; Bartlett, R. J. *Chem. Phys. Lett.* **1993**, *209*, 547. (c) Gutbrod, R.; Schondler, R. N.; Kraka, E.; Cremer, D. *Chem. Phys. Lett.* **1996**, *252*, 221.
(24) Cremer, D. *J. Chem. Phys.* **1979**, *70*, 1911.
(25) Lei, W.; Derecskei-Kovacs, A.; Zhang, R. *J. Chem. Phys.* **2000**, 113, 5354.
(26) Lei, W.; Zhang, R. *J. Chem. Phys.* **2000**, *113*, 153. (b) Suh, I.; Lei, W.; Zhang, R. *J. Phys. Chem.* **2001**, *105*, 6471.
(27) Cremer, D.; Pople, J. A. *J. Am. Chem. Soc.* **1975**, *97*, 1354. (b) Cremer, D. *Isr. J. Chem.* **1980**, *20*, 12.

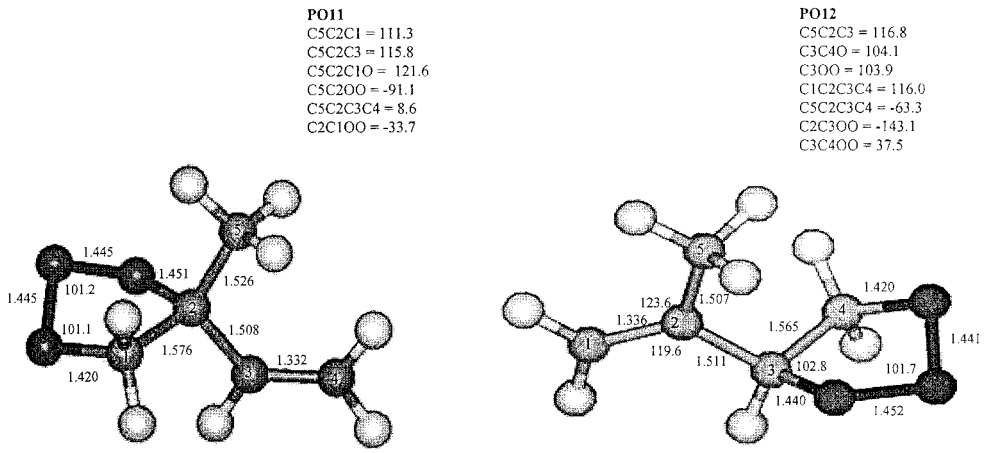

Figure 1. Equilibrium geometries of the lowest-energy conformers of the primary ozonides arising from the O_3–isoprene reaction calculated at the B3LYP/6-31G(d,p) level of theory (bond lengths in angstroms and angles in degrees).

correspond to the C_s symmetrical envelope (O-envelope), while ϕ values of 36° and 72° indicate the O-adjunct-envelope and C-envelope, respectively. Our calculations indicated that the lowest energy geometry of the primary ozonides resembles the O-envelope conformation. Optimization at the B3LYP/6-31G(d,p) level of theory for assumed starting geometries of the O-adjacent-envelope and C-envelope collapsed without activation to the O-envelope. For the analogous O_3–ethene reaction, the conformational nature of the primary ozonide 1,2,3-trioxolane has been determined to be the O-envelope by ab initio calculations,[28] and the theoretical predictions were consistent with experimental microwave study, which found the O-envelope as the only conformation in the gas phase.[29]

The energies of the primary ozonides were determined by using the B3LYP/6-31G(d,p) optimized geometries and the MP2 and CCSD(T) methods for single-point energy calculations. The absolute energies along with the zero-point energies (ZPEs) for all species determined in this work are provided in the Supporting Information. The O_3–isoprene reaction energies are listed in Table 1. Table 1 indicates that the reaction energies of O_3 addition to isoprene calculated by using the various levels of theory are very different. The values predicted by B3LYP/6-31G(d,p) and CCSD(T)/6-31G(d) are comparable, but are higher than those predicted by using MP2. Also, the values determined by using MP2 and two different basis sets differ by 5.1−5.4 kcal mol^{-1}. At the CCSD(T)/6-31G(d) + CF level of theory, the primary ozonides are 48.1−47.3 kcal mol^{-1} more stable than the separate O_3 and isoprene. **PO11** is slightly more stable than **PO12**, but the difference in the relative stability of the two primary ozonides is relatively small (0.8 kcal mol^{-1}).

Table 1. O_3–isoprene Reaction Energies with Zero-Point Correction Included (kcal mol^{-1})

reaction	B3LYP/ 6-31G(d,p)	MP2/ 631G(d)	MP2/ 6-311++G(d,p)	CCSD(T)/ 6-31G(d)	CCSD(T)/ 6-31G(d) + CF
11	−53.1	−45.5	−40.4	−53.2	−48.1
12	−54.0	−45.2	−39.8	−52.8	−47.3
21a	−6.4	3.3	−2.1	−1.7	−7.1
21b	−4.5	3.6	−2.1	−1.0	−6.8
22	−13.6	−3.2	−8.3	−7.9	−13.0
23	−11.4	−1.1	−5.9	−5.7	−10.5
24	−6.8	2.5	−3.7	−2.7	−8.8
25	−4.5	4.5	−0.7	−0.5	−5.7
26	−12.2	−1.2	−6.2	−6.7	−11.6
27	−11.6	−0.7	−5.7	−5.3	−10.3
28	−3.8	6.0	0.1	−0.1	−5.9
29	−6.1	3.0	−2.5	−1.7	−7.1
31a	−23.2	−34.5	−32.0	−26.5	−24.0
31b	9.6	10.3	6.2	10.9	6.9
31c	−16.0	−24.3	−27.3	−21.3	−24.3
32a	−14.0	−28.2	−25.9	−20.5	−18.2
32b	−9.0	−14.8	−18.8	−9.7	−13.7
32c	16.9	35.0	31.6	15.3	12.0
33a	−16.2	−30.3	−28.3	−22.7	−20.7
33b	−0.3	−4.4	−8.3	0.6	**−3.3**
33c	20.7	32.1	28.3	16.2	12.3
34a	−17.6	−31.6	−28.8	−23.3	−20.5
34b	13.4	11.3	7.3	13.5	9.4
34c	−14.8	−16.5	−19.8	−19.2	−22.5
35a	−19.9	−33.6	−31.7	−25.6	−23.6
35b	1.5	−5.8	−8.4	1.8	−0.8
35c	−6.9	5.8	1.1	−9.3	−14.0
36a	−14.0	−29.2	−27.0	−20.8	−18.5
36b	−12.4	−17.9	−22.2	−12.1	−16.4
36c	17.7	34.7	32.0	15.5	12.8
37a	−14.6	−29.7	−27.4	−22.2	−19.9
37b	18.9	6.5	3.2	15.1	11.8
37c	4.4	20.2	16.2	3.0	−1.0
38a	−17.6	−32.0	−29.5	−23.0	−20.6
38b	13.0	10.9	6.3	13.5	9.0
38c	−15.4	−20.3	−23.7	−20.1	−23.5
39a	−15.2	−29.0	−27.0	−21.5	−19.4
39b	9.8	−0.2	−3.4	8.2	5.0
39c	13.7	29.8	25.9	10.6	6.8

Transition States of Primary Ozonide Formation. Two transition states (**TS11** and **TS12**) were identified associated with O_3 addition to isoprene to form the primary ozonides. The transition states were searched using constrained geometry optimization at fixed C−O bond lengths using B3LYP/3-21G(d). We first considered the equilibrium structures of the primary ozonides as the initial guess for the transition states. The two C−O bond lengths were then successfully increased by a fixed increment relative to the equilibrium C−O bond length of the primary ozonide. Once a transition state was located, the geometry was optimized at the B3LYP/6-31G(d,p) level of theory. The transition-state structures were verified from the frequency calculations. For the two transition states identified, the calculated vibrational frequencies contained only one imaginary component, confirming the first-order saddle point configuration. The predicted transition-state structures are shown in Figure 2. We found that the structures of **TS11** and **TS12** also resemble the O-envelope conformation. The C−O distances of the transition states are between 2.21 and 2.49 Å, 0.76−1.07 Å longer than those of the corresponding primary ozonides.

(28) McKee, M. L.; Rohlfing, C. M. *J. Am. Chem. Soc.* **1989**, *111*, 2497.
(29) Zozom, J.; Gillies, C. W.; Suenram, R. D.; Lovas, F. J. *Chem. Phys.* **1987**, *139*, 64. (b) Gillies, J. Z.; Gillies, C. W.; Suenram, R. D.; Lovas, F. J. *J. Am. Chem. Soc.* **1988**, *110*, 7991.

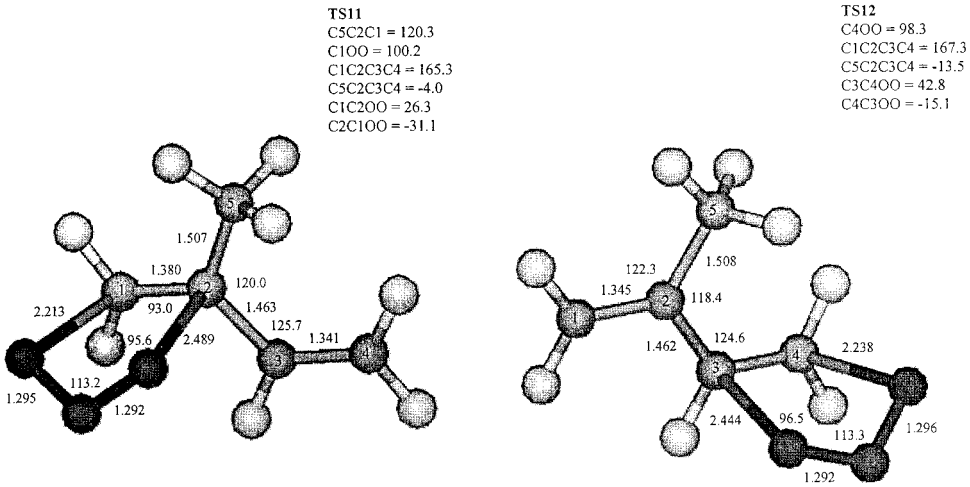

Figure 2. Same as Figure 1 except for the geometries of the transition states associated with the primary ozonide formation.

Table 2. O_3–isoprene Activation Energies with Zero-Point Correction Included (kcal mol^{-1})

reaction	B3LYP/ 6-31G(d,p)	MP2/ 6-31G(d)	MP2/ 6-311++G(d,p)	CCSD(T)/ 6-31G(d)	CCSD(T)/ 6-31G(d) + CF
11	−1.6	−5.5	−4.8	2.6	3.3
12	−2.3	−6.1	−4.8	2.1	3.4
21a	16.8	4.5	0.5	17.9	14.0
21b	15.3	4.2	−0.5	16.8	12.2
22	13.4	2.6	−1.4	15.4	11.3
23	14.2	3.9	−0.2	16.4	12.3
24	14.3	4.6	0.0	16.8	12.3
25	17.8	7.1	3.1	19.6	15.6
26	14.1	3.1	−0.8	15.9	11.9
27	15.4	4.7	0.3	17.5	13.1
28	15.8	6.1	1.5	18.3	13.7
29	18.4	8.0	3.2	20.7	15.9
31a	20.6	23.3	24.0	19.1	19.8
31b	31.7	31.2	29.2	34.0	32.0
32a	23.3	25.0	25.5	21.6	22.1
32b	16.5	15.8	13.3	21.3	18.8
32c	44.9	33.7	28.9	25.1	20.3
33a	18.6	21.0	21.2	17.3	17.5
33b	19.5	19.1	16.3	24.6	21.9
34a	17.8	19.4	19.5	16.6	16.7
34b	31.1	28.9	27.1	33.0	31.2
35a	18.3	20.4	20.5	16.7	16.9
35b	34.8	37.2	30.2	43.1	36.2
36a	20.5	21.7	21.9	19.3	19.5
36b	16.0	15.2	12.7	20.9	18.4
36c	45.6	33.3	28.8	25.5	21.0
37a	23.6	25.3	25.9	21.6	22.2
38a	15.7	17.5	17.3	14.7	14.5
38b	31.6	29.2	27.1	33.6	31.6
39a	26.6	28.9	30.1	24.2	25.5

Cycloaddition of O_3 to isoprene likely occurs through a van der Waals complex prior to the transition state:

$$C_5H_8 + O_3 \leftrightarrow [C_5H_8\cdots O_3] \rightarrow PO \quad (1)$$

The net activation energy of the overall reaction 1 is expressed by

$$E_a = E_b - E_r = (E_{ts} - E_c) - (E_{reactants} - E_c) = E_{ts} - E_{reactants} \quad (2)$$

where E_b and E_r are the respective activation energies for the backward and forward reactions of the complex and E_{ts}, E_c, and $E_{reactants}$ are the respective energies of the transition state, the complex, and the reactants. The net activation energies for the primary ozonide formation are provided in Table 2. The results show that the activation energies of O_3 addition to isoprene are very sensitive to effects of electron correlation and basis set. Both B3LYP and MP2 produce negative values for the activation energies, which apparently correspond to unreliable barriers for the O_3-addition reactions. The activation energies predicted by the CCSD(T)/6-31G(d) method are 2.6 kcal mol^{-1} for **TS11** and 2.1 kcal mol^{-1} for **TS12**. We also employed the basis set correction method discussed above to determine the activation energies of the O_3–isoprene reaction, by correcting the CCSD(T)/6-31G(d) energies with the correction factors developed at the MP2 level of theory. The activation energies obtained at the CCSD(T)/6-31G(d) + CF level of theory are 3.3 kcal mol^{-1} for **TS11** and 3.4 kcal mol^{-1} for **TS12**.

Previous theoretical studies of ozonolysis of ethene have indicated that the transition state associated with the O_3 addition to ethene was not found at the B3LYP/6-31G(d,p) level.[17,30] It is well-known that the DFT method fails in the case of a van der Waals complex and loose transition states.[31] The energy of the ozone−ethene van der Waals complex is erroneously predicted using B3LYP, and the barrier of the ozone−ethene cycloaddition is calculated to be only 0.2 kcal mol^{-1}, which is largely underestimated. On the other hand, a barrier height of 3.5 kcal mol^{-1} for O_3 addition to ethene was determined using MP2/6-31G(d,p) and MP4/6-31G(d,p).[17] Our activation energies of the O_3–isoprene reaction determined using CCSD(T)/6-31G(d) + CF are similar to those reported previously for the O_3–ethene reaction using the MP2 or MP4 method, which is expected to be typical of the general type of the O_3–alkene reactions. Several experimental studies have investigated the temperature-dependent rate constants of the O_3–isoprene reaction.[3,32] On the basis of the experimental studies, the activation energy of O_3 addition to isoprene is inferred to be in the range of 3.8−4.2 kcal mol^{-1}, consistent with our calculated values using CCSD(T)/6-31G(d) + CF.

Cleavage of Primary Ozonides. In this study we considered only the concerted mechanism for cleavage of the primary ozonides. Concerted decomposition of the O_3–isoprene primary

(30) Gillies, C. W.; Gillies, J. Z.; Suenram, R. D.; Lovas, F. J.; Kraka, E.; Cremer, D. *J. Am. Chem. Soc.* **1991**, *113*, 2412.
(31) Jones, R. O.; Gunnarsson, O. *Rev. Mod. Phys.* **1989**, *61*, 681. (b) Kristyan, S.; Pulay, P. *Chem. Phys. Lett.* **1994**, *229*, 175. (c) Anderson, Y.; Langreth, D. C.; Gonzales, C. A.; Gill, P. M. W.; Pople, J. A. *Chem. Phys. Lett.* **1994**, *221*, 100.
(32) Adeniji, S. A.; Kerr, J. A.; Williams, M. R. *Int. J. Chem. Kinet.* **1981**, *13*, 209. (b) Atkinson, R.; Winer, A. M.; Pitts, J. N. Jr. *Atmos. Environ.* **1982**, *16*, 1017. (c) Treacy J.; Hag, M. El.; O'Farrell, D.; Sidebottom, H. *Ber. Bunsen-Ges. Phys. Chem.* **1992**, *96*, 422. (d) Khamaganov, V. G.; Hite, R. A. *J. Phys. Chem.* **2001**, *105*, 815.

ozonides occurs with cleavage of either the C−O bonds or the O−O bonds, each pathway forming a stable aldehyde or ketone, along with a carbonyl oxide (Criegee intermediate). The primary ozonide **PO11** decomposes to form methyl vinyl ketone or formaldehyde; for **PO12**, the stable products are methacrolein or formaldehyde. The carbonyl oxides are classified as syn or anti conformations, referring to the position of the 2-propenyl or methyl substituent with respect to the COO unit. As is shown in Scheme 1, decomposition of the primary ozonides yields five possible steroisomers of the carbonyl oxides, consisting of syn (i.e., **CI2**, **CI5**, **CI6**, and **CI9**) or anti (**CI3**, **CI4**, **CI7**, and **CI8**) configurations. Alternatively, the carbonyl oxides can also be identified as the cis (**CI2**, **CI3**, **CI4**, and **CI5)** or trans (**CI6**, **CI7**, **CI8**, and **CI9**) conformations, referring to the position of the vinyl group with respect to the COO unit.

Transition-state search for cleavage of the primary ozonides was also performed by using the constrained geometry optimization procedure as discussed above. Ten transition states were identified associated with the decomposition of the primary ozonides to form **CI1**−**CI9**. Calculations using the intrinsic reaction coordinate (IRC) method were performed for each transition state, showing that each TS corresponded to a unique product (**CI1**−**CI9**). For example, for **TS22** the IRC calculation confirmed **CI2** as the product. Geometries of the transition states for the primary ozonide decomposition are depicted in Figure 3. Cleavage of the envelope conformations of the primary ozonides occurs via a strongly bent envelope-looking transition state. The lengths for breaking the C−O and C−C bonds at the transition states are in the ranges of 2.01−2.08 and 1.88−1.92 Å, respectively.

The relative energies of the transition states of cleavage of the primary ozonides are presented in Table 3. Table 3 indicates that the relative energies obtained by using B3LYP/6-31G(d,p) and CCSD(T)/6-31G(d) + CF are slightly different, with a largest difference of 1.7 kcal mol^{-1} between the two methods. The relative stability predicted by the two methods, however, is nearly identical: **TS22** is the most stable structure, and **TS29** is the least stable form. At the CCSD(T)/6-31G(d) + CF level of theory, the **TS22** structure is 5.3 kcal mol^{-1} more stable than **TS29**. The activation energies for cleavage of the primary ozonides are also given in Table 3. It is apparent from the table that the MP2 method substantially underestimated the barriers, compared to the values predicted by B3LYP and CCSD(T). The decomposition energies of the primary ozonides obtained with B3LYP/6-31G(d,p) were systematically smaller than those produced by CCSD(T)/6-31G(d), but inclusion of the basis set factor CF lowered the CCSD(T) barriers. The differences in the barriers predicted by B3LYP/6-31G(d,p) and CCSD(T)/6-31G(d) + CF range from 1.9 to 3.1 kcal mol^{-1}. At the CCSD(T)/6-31G(d) + CF level of theory, the decomposition barriers of the primary ozonides are between 11.3 and 15.9 kcal mol^{-1}. At all levels of theory (except for MP2/6-311++G(d,p)) cleavage of **PO11** via the transition state **TS22** is most favorable, while cleavage of **PO12** via the transition state **TS21b** or **TS24** is more preferential. The relative energies of the stationary points located on the singlet ground-state primary ozonide potential energy surface calculated using CCSD(T)/6-31G(d) + CF are shown in Figure 4.

Carbonyl Oxides. The geometries of the lowest energy conformers of the carbonyl oxides **CI1**−**CI9** are shown in Figure 5. In Table 3, the relative energies of the carbonyl oxides are also given at the B3LYP/6-31G(d,p) and CCSD(T)/6-31G(d) + CF levels of theory. Also included in Table 3 for comparison are the relative energies reported by Gutbrod et al.[16] Our calculated relative energies using B3LYP/6-31G(d,p) agree well with those obtained by Gutbrod, but the values obtained using CCSD(T)/6-31G(d) + CF are slightly different, with the largest difference of 1.1 kcal mol^{-1} for **CI8** between the two methods. The relative stability of the carbonyl oxides predicted by B3LYP and CCSD(T) is, however, similar. It is seen from Table 3 that **CI2**, **CI3**, **CI6**, and **CI7** (group I) are more stable than **CI4**, **CI5**, **CI8**, and **CI9** (group II). In addition, the syn **CI2** configuration is most stable within group I, while the anti **CI4** configuration is most stable within group II. The relative stability of the carbonyl oxides can be explained in terms of conjugative, hyperconjugative, H-bonding, and steric interactions. The methyl substituent for the species within group I is located at the COO unit and corresponds to a stabilizing hyperconjugative effect, which explains the greater stability for this group. Attractive interactions between the positively charged H atom and the negatively charged terminal O atom further improve the stability for **CI2**, **CI5**, **CI6**, and **CI9**. Alternatively, 4-electron destabilization effects are responsible for lowering the stability for the cis configurations of **CI6** and **CI8** with respect to their corresponding trans forms of **CI2** and **CI4**, respectively. A comparison of the relative stability of the carbonyl oxides and their corresponding transition states for cleavage of the primary ozonides (Table 3) reveals that there is a similarity: the more stable carbonyl oxides generally correspond to more stable forms in the transition states. This indicates that electronic and steric effects of the methyl or vinyl group are also reflected in the corresponding transition-state geometries. As in Table 1, the decomposition energies of the primary ozonides to form the carbonyl oxides are in the range of −5.7 to −13.0 kcal mol^{-1} at the CCSD(T)/6-31G(d) + CF level of theory.

Unimolecular Reactions of Carbonyl Oxides. The carbonyl oxides formed from cleavage of the primary ozonides of the O_3–isoprene reaction will either decompose to yield OH or undergo rearrangement to form the more stable isomer dioxirane. Decomposition of the carbonyl oxides occurs via H-migration to form a hydroperoxide intermediate, which subsequently dissociates to form OH and formyl radicals. Among the nine carbonyl oxides, **CI1**, **CI4**, and **CI8** possess C4-type H atoms, and **CI2** and **CI6** possess A5 H atoms. Migration of a methyl H of **CI5** leads to a six-membered transition, and the H atom is denoted as A6. **CI3**, **CI7**, and **CI9** possess a vinyl H atom that migrates via a five-membered (V5-type H atom) or six-membered (V6-type H atom) transition state. We performed calculations to obtain the equilibrium structures of dioxirane, hydroperoxide, and formyl radicals. The transition states corresponding to the unimolecular reactions of the carbonyl oxides were also identified. Figure 6 shows the geometries of selected dioxirane (**DIO**), hydroperoxide (**HP**), and formyl radical (**RCO**) along with the corresponding transition states determined at the B3LYP/6-31G(d,p) level of theory. Our predicted geometries for the various species associated with the unimo-

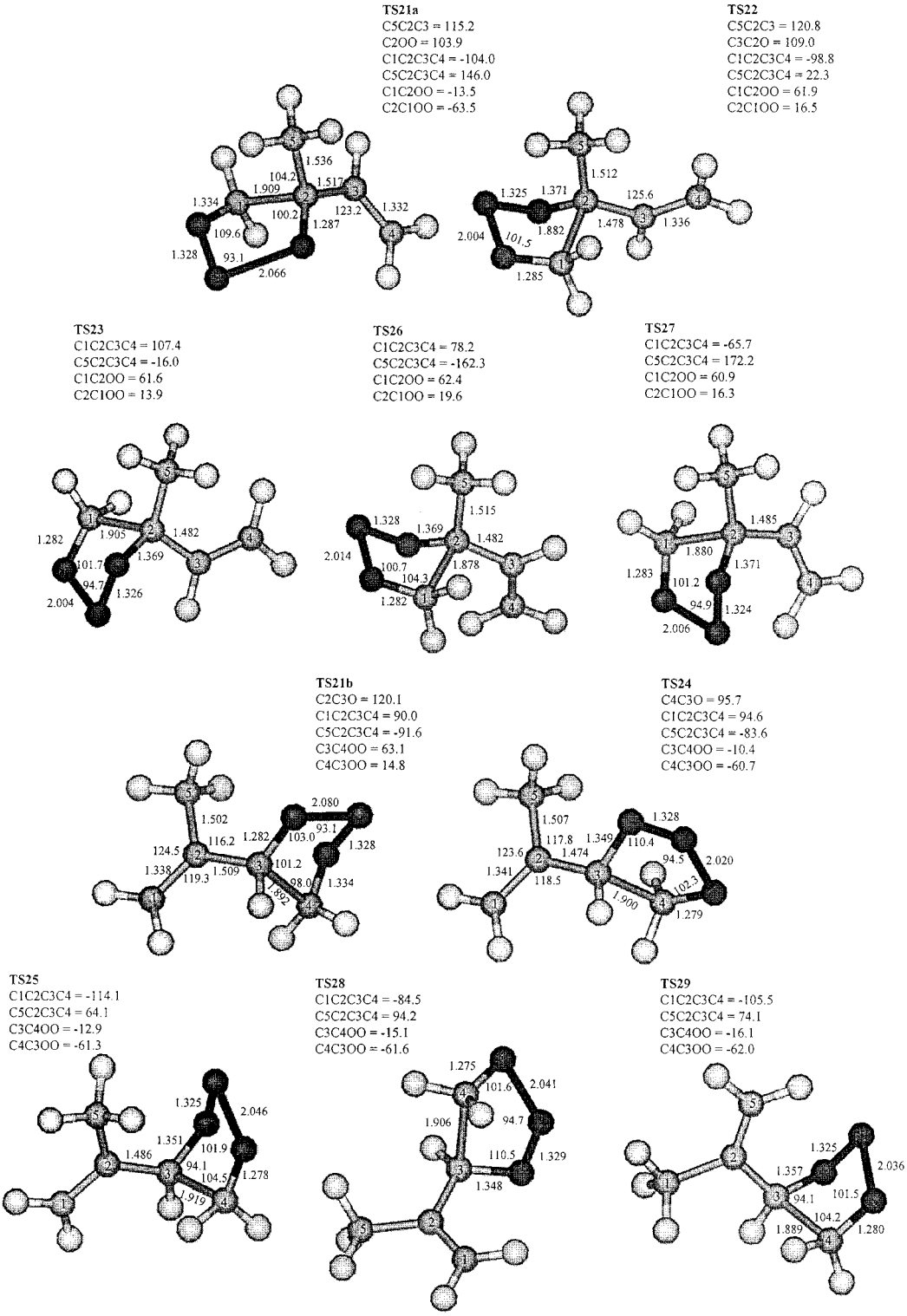

Figure 3. Same as Figure 1 except for the geometries of the transition states associated with cleavage of the primary ozonides.

lecular reactions of the carbonyl oxides are generally in agreement with those reported by Gutbrod et al.[16]

The reaction and activation energies of the unimolecular reactions of the carbonyl oxides are also contained in Tables 1 and 2, respectively. It is seen from the two tables that effects of electron correlation and basis set produce noticeable differences in the calculated energetics. At the B3LYP/6-31G(d) level of theory, our calculated barriers are generally similar to those reported by Gutbrod et al.,[16] except in a few cases where significant differences exist between the two studies. For example, we predict a barrier of 15.7 kcal mol^{-1} for **CI8** isomerization to dioxirane (R38a), 8.6 kcal mol^{-1} smaller than the value determined by Gutbrod et al. Since the comparison is made by employing the same level of theory in the energy calculations, a difference in the activation energy of such magnitude is not anticipated. The origin of this disparity is

Table 3. Relative Energies (kcal mol^{-1}) of the Carbonyl Oxides and Their Corresponding Transition States of Cleavage of the Primary Ozonides

CI	ΔE^a	ΔE^b	ΔE^c	TS	ΔE^d	ΔE^e
CI2	0	0	0	**TS22**	0	0
CI3	2.2	2.2	2.5	**TS23**	1.0	1.2
CI4	5.9	5.9	5.0	**TS24**	0.1	1.6
CI5	7.9	7.9	7.8	**TS25**	3.2	4.8
CI6	1.5	1.5	1.5	**TS26**	0.8	0.7
CI7	2.0	1.9	2.7	**TS27**	2.3	2.1
CI8	9.1	9.1	8.0	**TS28**	1.6	3.2
CI9	6.4	6.4	6.5	**TS29**	4.1	5.3

[a] Relative energies to **CI2** at the B3LYP/6-31G(d,p) level. [b] Relative energy data from Gutbrod et al.[16] at the B3LYP/6-31G(d,p) level. [c] Relative energies at the CCSD(T)/6-31G(d) + CF level. [d] Relative energies to **TS22** at the B3LYP/6-31G(d,p) level. [e] Relative energies at the CCSD(T)/6-31G(d) + CF level.

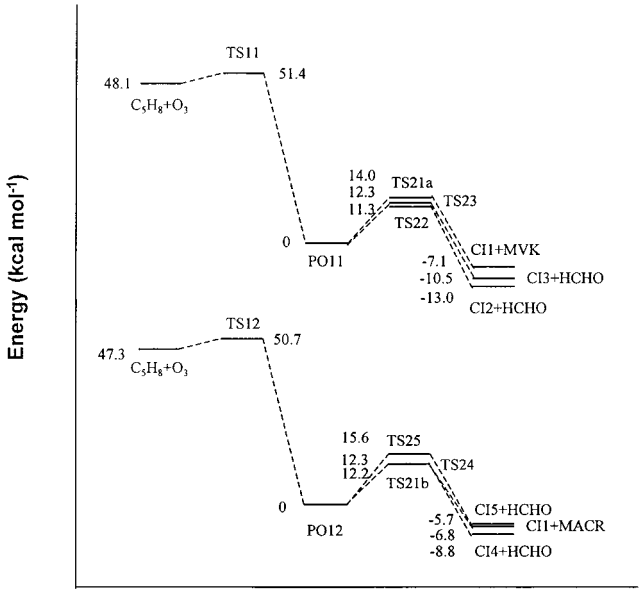

Figure 4. O_3–isoprene reaction coordinate: relative energies of the stationary points located on the primary ozonide ground-state potential energy surface. The energy values are given in kcal mol^{-1} and are calculated using CCSD(T)/6-31G(d) + CF//B3LYP/6-31G(d,p).

unclear. On the other hand, our calculated barrier using B3LYP/6-31G(d,p) differs only by 1.2 kcal mol^{-1} from the value obtained using CCSD(T)/6-31G(d) + CF.

Our results indicate that the carbonyl oxides with the C4-type H atoms (**CI1**, **CI4**, and **CH8**) have much higher barriers for H-migration to form hydroperoxide (R3b) than for cyclization to form dioxirane (R3a). The difference in the barriers between R3a and R3b is in the range of 12.2−17.1 kcal mol^{-1} using CCSD(T)/6-31G(d) + CF. The higher barriers for H-migration of these carbonyl oxides can be explained by the fact that the unstable singlet carbenes are formed, leading to high-lying transition states. For the carbonyl oxides possessing A6-, V5-, or V6-type H atom (**CI3**, **CI5**, **CI7**, and **CI9**), H-migration leads to the formation of singlet biradicals which are highly unstable. We were unable to determine the structures of those biradicals at the B3LYP/6-31G(d,p) level of theory. Geometry optimization of the biradicals collapsed to the more stable isomeric forms **HP3**, **HP5**, **HP7**, and **HP9** (their structures are provided in the Supporting Information). On the other hand, we identified the transition states corresponding to H-migration for **CI3** and **CI5**. The activation energies of R33b and R36b are 21.9 and 36.2 kcal mol^{-1} at the CCSD(T)/6-31G-(d) + CF level of theory, respectively. These values are 4.4 and 19.3 kcal mol^{-1} higher than the corresponding barriers for dioxirane formation. Transition-state search for H-migration of **CI7** and **CI9** was unsuccessful. Nevertheless, the barriers for H-migration of **CI7** and **CI9** should be significantly higher than for isomerization to dioxirane. Gutbrod et al. also concluded that there is a negligible probability of OH formation from the two carbonyl oxides.[16] For the case of the carbonyl oxides with A5 H atoms (**CI2** and **CI6**), facile H-migration takes place as a result of close interaction between the methyl H atom and the terminal O atom. The predicted barriers using CCSD(T)/6-31G-(d) + CF are 18.8 kcal mol^{-1} for R32b and 18.4 kcal mol^{-1} for R36b, 3.3 and 1.1 kcal mol^{-1} lower than the corresponding values for dioxirane formation. For the two hydroperoxides **HP2** and **HP6** formed from reactions R32b and R36b, the former is 2.2 kcal mol^{-1} more stable than the latter. Decomposition of **HP2** and **HP6** requires 21.3 and 20.3 kcal mol^{-1} at the CCSD-(T)/6-31G(d) + CF level of theory, respectively. Gutbrod et al.[16] determined a barrier of 10.3 kcal mol^{-1} for the decomposition of **HP6** using B3LYP/6-31G(d,p), which is significantly lower than our value. Figure 7 illustrates the relative energies of the stationary points located on the singlet ground-state potential energy surface of selected carbonyl oxides at the CCSD(T)/6-31G(d) + CF level of theory.

High-Level Ab Initio Calculations. In an effort to validate the basis set correction approach, we have carried out additional calculations employing higher levels of ab intio theory, including CCSD(T)/6-311G(d,p). In addition, the Gaussian-2 (G2) theory[33,34] was used to evaluate the activation energies for the unimolecular reactions of **CI1**, **CI2**, **CI3**, and **CI6**. The G2 theory is a composite method, based on the 6-311G(d,p) basis set and several basis extensions. Treatment of electron correlation is by Møller−Plesset purturbation theory and quadratic configuration interaction (QCI). The final energies are effectively at the QCISD(T)/6-311+G(3df,2p) level. It has been suggested that the G2 method produces the least mean absolute deviation (MAD) error compared to the other Gaussian theories (i.e., G1, G2(MP2), and G2(MP2,SVP)).[34]

The results of the high-level ab initio calculations are summarized in Table 4. The activation energies determined by using CCSD(T)/6-31G(d) + CF and CCSD(T)/6-311G(d,p) are very similar, with a largest difference of 1.0 kcal mol^{-1} for R33b. The methods of CCSD(T)/6-311G(d,p) and QCISD(T)/6-311G-(d,p) also produce consistent activation energies within 0.5 kcal mol^{-1}. Except for R31a (in which case the activation energy differs by 2.6 kcal mol^{-1}), the activation energies predicted by using CCSD(T)/6-311G(d,p) and G2 agree within 1.1 kcal mol^{-1}. In addition, the activation energies calculated by using G1 and G2 are also similar, except for the case of R33b in which the activation energy calculated with G1 is 2.5 kcal mol^{-1} higher than that calculated by using the G2 method. Two recent studies have also pointed out the importance of using high-level ab initio theory in the energy calculations of the carbonyl oxides.[18,21] Cremer et al. calculated the barrier for R31a using CCSD(T)/6-311G(d,p)//B3LYP/6-311+G(3df,3pd), yielding a value of 20.1 kcal mol^{-1}.[18] Using the method of CCSD(T)/6-311G(d,p)//B3LYP/6-31G(d,p), Aplincourt et al.[21] determined a barrier of

(33) Curtiss, L. A.; Raghavachari, K.; Trucks, W. G.; Pople, J. A. *J. Chem. Phys.* **1991**, *94*, 7221. (b) Curtiss, L. A.; Raghavachari, K.; Redfern, P. C.; Pople, J. A. *J. Chem. Phys.* **1996**, *106*, 1063.
(34) Jensen, F. *Introduction to Computational Chemistry*; John Wiley & Sons: New York, 1999.

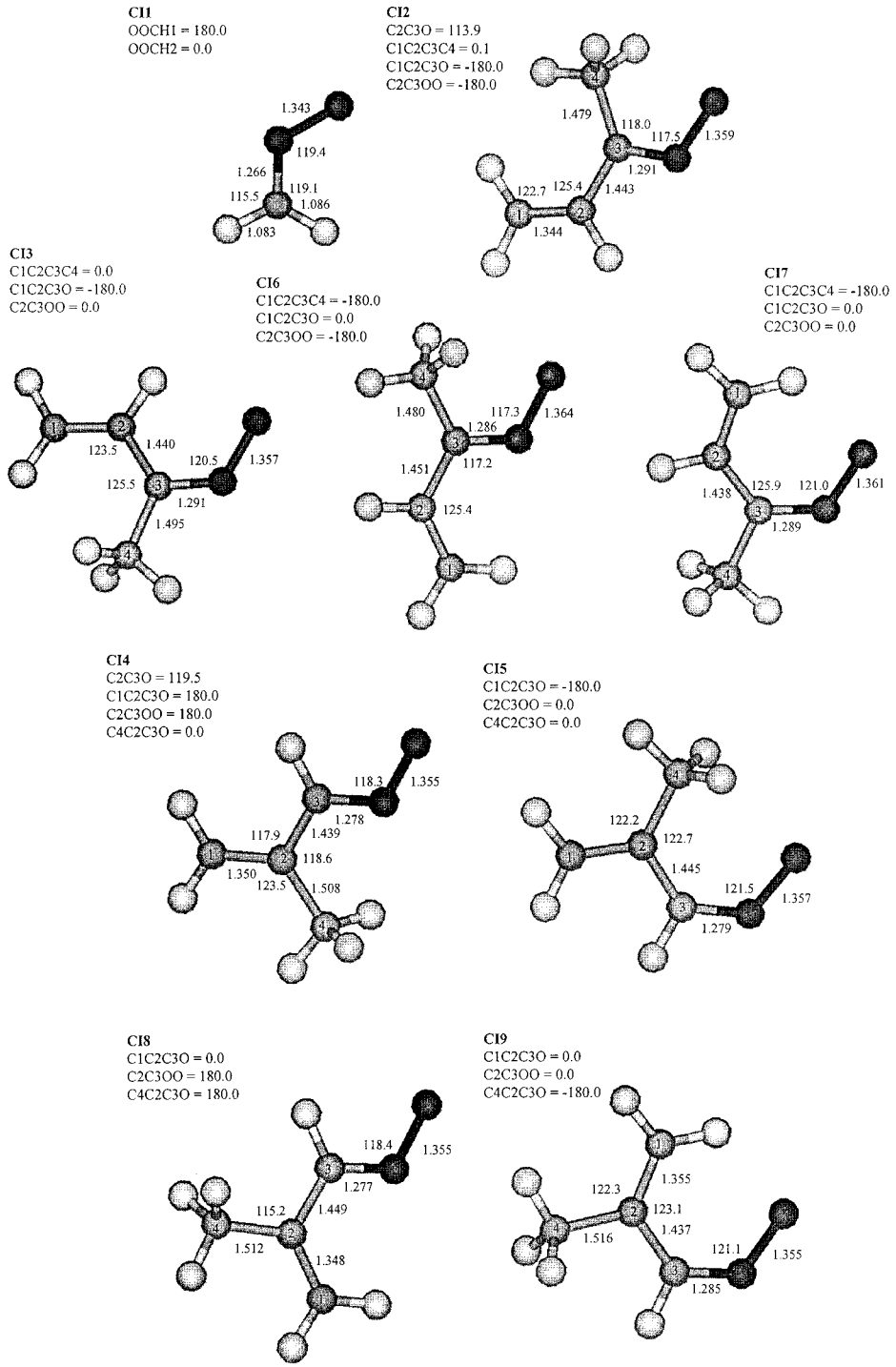

Figure 5. Same as Figure 1 except for the equilibrium geometries of the carbonyl oxides.

19.8 kcal mol^{-1} for the same reaction. Our calculated activation energy for R31a is consistent with the two previous studies. Hence, the results presented in Table 4 confirm the accuracy of the energetics predicted using the basis set correction factor. In the kinetic calculations we employed mainly the CCSD(T)/6-31G(d) + CF energetics.

Kinetic Calculations. We have calculated the rate constant for the O_3–isoprene reaction using transition-state theory (TST). The high-pressure-limit unimolecular rate constant is expressed by[35]

$$k_{\text{uni}} = \frac{kT}{h}\frac{Q^{\ddagger}}{Q}\exp\left(-\frac{E_a}{kT}\right) \qquad (3)$$

where $Q^{\ddagger}$ is the partition function of the transition state with the vibrational frequency corresponding to the reaction coordinate removed, Q is the partition function of the reactant, and E_a is the zero-point corrected activation energy defined by eq 2. Using the presently obtained geometries and energetics, we obtained TST rate constants of 9.3×10^{-18} and 6.5×10^{-18}

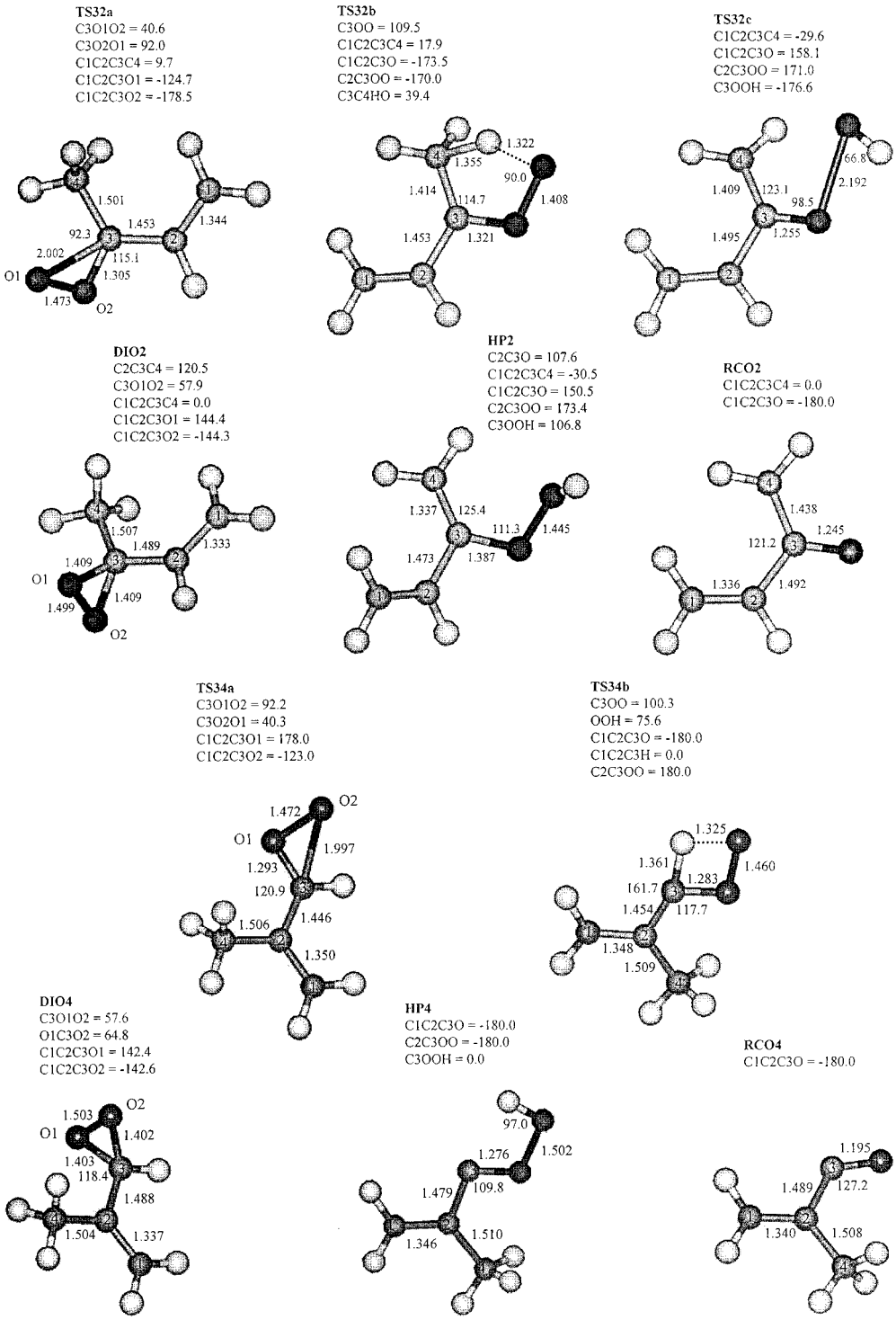

Figure 6. Same as Figure 1 except for the geometries of selected dioxirane, hydroperoxide, and formyl radical and their corresponding transition states.

cm^3 $molecule^{-1}$ s^{-1} for R11 and R12 at 300 K. The calculated overall rate of 1.58×10^{-17} cm^3 $molecule^{-1}$ s^{-1} is in marked agreement with the experimentally measured value (1.43×10^{-17} cm^3 $molecule^{-1}$ s^{-1}).[3,32] Since there are no adjustable parameters in calculating the TST rate constant, the success in reproducing the experimental rate suggests that the ab initio energetics obtained using CCSD(T)/6-31G(d) + CF provide an accurate description of the salient features of the O_3–isoprene reaction.

Our results reveal a branching ratio of 0.59:0.41 between **PO11** and **PO12**, implying that the initial two O_3 addition pathways are nearly equally accessible. In the previous study by Gutbrod et al.[16] it was suggested that O_3 attack of isoprene occurs preferentially at the methyl-substituted double bond, on the basis of the consideration that electron-rich double bonds (double bonds with a higher π HOMO) form a stronger π complex with O_3 and hence are more prone to undergo the

(35) Lei, W.; Zhang, R.; McGivern, W. S.; Derecskei-Kovacs, A.; North, S. W. *J. Phys. Chem.* **2001**, *105*, 471. (b) Lei, W.; Zhang, R. *J. Phys. Chem.* **2001**, *105*, 3808. (c) Lei, W.; Zhang, R.; McGivern, W. S.; Derecskei-Kovacs, A.; North, S. W. *Chem. Phys. Lett.* **2000**, *326*, 109.

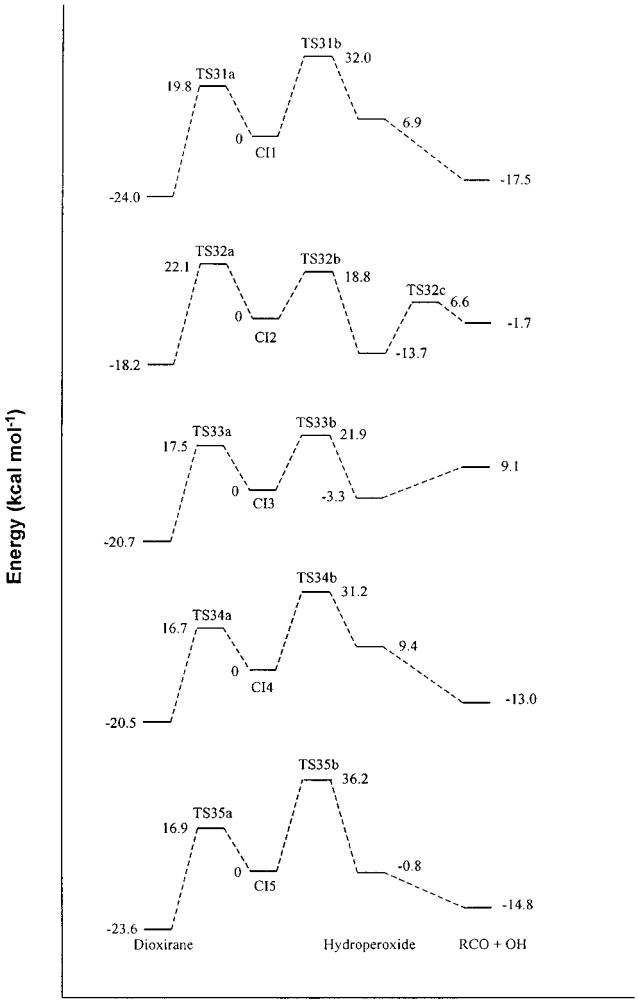

Figure 7. Same as Figure 4 except for the relative energies of the stationary points located on the singlet ground-state potential energy surface of selected carbonyl oxides.

Table 4. High-Level ab Initio Calculations of Activation Energies (kcal mol^{-1}) for the Unimolecular Reactions of the Carbonyl Oxides with ZPE Included

reaction	CCSD(T)/ 6-31G(d)	CCSD(T)/ 6-31G(d) + CF	CCSD(T)/ 6-311G(d,p)	QCISD(T)/ 6-311G(d,p)	G1	G2
31a	19.1	19.8	19.9	19.4	17.2	17.2
31b	34.0	32.0	31.1	31.4	32.1	32.0
32a	21.6	22.1	22.5	22.9	21.1	21.4
32b	21.3	18.8	18.0	18.2	18.4	19.1
33a	17.3	17.5	18.0	18.0	16.0	16.5
33b	24.6	21.9	20.9	21.1	25.5	23.0
36a	19.3	19.5	20.3	20.5	18.3	18.7
36b	20.9	18.4	17.7	17.9	18.1	18.9

cycloaddition reaction to primary ozonide. Our rate calculation predicts a comparable relative branching ratio between **PO11** and **PO12**, with the O_3 addition to the substituted double bond being only slightly more favorable than that to the unsubstituted double bond. Hence, both O_3 addition pathways need to be accounted for when OH formation from the O_3–isoprene reactions is determined.

To assess the fate of the chemically excited primary ozonide and carbonyl oxide, we evaluated their stabilization, isomerization, and decomposition using a statistical-dynamical master equation. The same approach has been recently employed to predict the OH yields from ozonolysis of a number of symmetric alkenes,[17,20] and the calculated OH yields compare favorably

Table 5. Relative Branching Ratios of Isomerization, Decomposition, and Stabilization of the Excited Carbonyl Oxide at 1013 mb and High-Pressure-Limit Unimolecular Rate Constants of Stabilized Carbonyl Oxides[a]

	branching ratio			k (s^{-1})	
species	dioxirane	OH	stabilization	dioxirane	OH
CI1	0.05	~0.0	0.95	2.4×10^{-2}	1.2×10^{-12}
CI2	0.08	0.38	0.54	3.2×10^{-4}	6.6×10^{-2}
CI3	0.60	0.06	0.34	6.2×10^{-1}	6.9×10^{-4}
CI6	0.18	0.35	0.47	1.8×10^{-2}	1.1×10^{-1}

[a] All calculations were performed at 300 K using the energetics obtained at the CCSD(T)/6-31G(d) + CF//B3LYP/6-31G(d,p) level of theory.

with the experiments.[20] Briefly, the concentration of a species formed by chemical activation is related to the balance over all gain and loss processes[17,20]

$$\frac{dn_i}{dt} = Rf_i - \omega n_i + \sum_j P_{ij} n_j - \sum_r k_{ri} n_i \qquad (4)$$

where n_i is the concentration of the intermediate having internal energy E_i, R is the overall formation rate, f_i is the normalized energy distribution, P_{ij} is the energy transfer probability from j to i, k_{ri} is the reaction rate constant for pathway r, and ω is the collision frequency.[36] Assuming the steady-state condition, $dn_i/dt = 0$, eq 4 becomes

$$R\mathbf{F} = [\omega(\mathbf{I} - \mathbf{P}) + \sum \mathbf{K}_r]\mathbf{N}^s \equiv \mathbf{J}\mathbf{N}^s \qquad (5)$$

where the vector/matrix symbols correspond to those in eq 4 and **I** denotes the unit matrix. The steady-state population $\mathbf{N}^s$ follows from $\mathbf{N}^s = R\mathbf{J}^{-1}\mathbf{F}$, and the rate of reaction r is $D_r = \sum(\mathbf{K}_r\mathbf{N}^s)_i$. The relative yields are then expressed by $D_r/R = \sum(\mathbf{K}_r\mathbf{J}^{-1}\mathbf{F})_i$, and the stabilization fraction follows from $S/R = 1 - \sum D_r/R$. In all calculations reported in this work, an energy grain size of 100 cm^{-1} is used, and the average energy change per collision is equal to 250 cm^{-1}.

The master equation analysis of **PO11** and **PO12** predicts negligible stabilization at 1013 mb. This is expected because of a large excess of the internal energy of the O_3 addition reaction. As discussed above, H-migration to form the hydroperoxide intermediate is favorable only for carbonyl oxides **CI2** and **CI6**, while for all others the barriers for H-migration are substantially higher than those of isomerization to form dioxirane so that there is less OH formation from the other carbonyl oxides. The branching ratios for the formation of **CI2**, **CI3**, and **CI6** from **PO11** decomposition are calculated to be 0.24, 0.19, and 0.24, respectively. Hence, dissociation of the excited primary ozonides leads to formation of syn and anti conformations each with a nonnegligible amount. For the carbonyl oxides, we have neglected the interconversion between the anti and syn configurations because of the existence of a large energy barrier.[37] The calculated relative product yields from the unimolecular reactions of the carbonyl oxide are summarized in Table 5. Table 5 indicates that a significant fraction of **CI2**, **CI3**, and **CI6** is collisionally stabilized, ranging from 0.34 to 0.54. Decomposition of the excited carbonyl oxides leads to

(36) Gilbert, R. G.; Smith, S. C. *Theory of unimolecular and recombination reactions*; Blackwell Scientific: Oxford, U.K., 1990. (b) Holbrook, K.; Pilling, M.; Robertson, S. *Unimolecular Reactions*; John Wiley & Sons Inc.: Chichester, U.K., 1996.
(37) Anglada, J. M.; Bofill, J. M.; Olivella, S.; Sole, A. *J. Am. Chem. Soc.* **1996**, *118*, 4636.

prompt OH formation, occurring on a very short time scale (less than 10^{-6} s based on the RRKM calculations). **CI2** and **CI6** preferentially dissociate to OH, but OH formation from **CI3** is much smaller, due to the higher barrier for H-migration than isomerization (by 4.4 kcal mol^{-1}). For **CI1**, our results indicate an exceedingly small OH yield, consistent with two previously theoretical predictions.[17,20] It is also interesting to note that the prompt OH yields from decomposition of **CI2** and **CI6** are nearly identical. **CI6** corresponds to the trans configuration of **CI2** (for the vinyl group with respect to the COO unit), and is 1.5 kcal mol^{-1} less stable than **CI2** (Table 3). We found that the inclusion of only the more stable cis or trans conformations of the carbonyl oxides from the decompositions of **PO11** and **PO12** in the master equation treatment does not produce a noticeably different OH yield compared to the case that differentiates the two forms.

To assess the fate of stabilized carbonyl oxides, we calculated the unimolecular rate constants for isomerization and decomposition using eq 3, which provides the high-pressure-limit rate constants due to thermal activation. Table 5 also contains the TST calculated high-pressure-limit rate constants of the two consecutive reactions of the carbonyl oxides **CI1**, **CI2**, **CI3**, and **CI6**. Similarly, stabilized **CI1** and **CI3** undergo predominantly isomerization to form dioxirane, whereas **CI2** and **CI6** have a higher rate of decomposition to form OH. A prominent feature is the relatively small rate constants of the unimolecular reactions of the thermalized carbonyl oxide. For **CI2**, the rate constant of H-migration to form hydroperoxide is 6.6×10^{-2} s^{-1}, corresponding to a lifetime of about 15 s. Hence, thermal OH formation occurs on a time scale significantly longer than that of prompt OH formation. Isomerization of **CI3** to form dioxirane is also slow; the lifetime of stabilized **CI3** is on the order of a fraction of a second.

In the absence of any carbonyl oxide scavenger, both excited and deactivated carbonyl oxides **CI2** and **CI6** decompose to form OH, even though the two processes take place on significantly different time scales. On combining the relative branching ratios for the primary ozonides and carbonyl oxides, we obtain an overall OH yield of 0.25 at atmospheric pressure, contributed by prompt (0.11) and thermal (0.14) OH formation. To survey the effect of the energetics on the OH yield, we performed additional calculations using the activation energies of the unimolecular reactions of the carbonyl oxides at the CCSD(T)/6-311G(d,p) level of theory (Table 4). The calculated OH yield differs by less than 2% from that using CCSD(T)/6-31G(d) + CF. Our calculations can be compared to the available experimental studies of OH formation. For the majority of the previous OH yield measurements, the experimental time scale well exceeds the thermal lifetime of the stabilized carbonyl oxides (i.e., about 15 s), so that the measured values also reflect prompt and thermal OH formation. Most experimentally measured OH yields range from 0.19 to 0.27 near atmospheric pressure,[12,16] with one exceptional value of 0.53 (ref 13). Hence, our predicted OH formation yield from the isoprene ozonolysis is consistent with most of the previous experimental results.

Conclusions

Our theoretical investigation reveals several important aspects of the isoprene ozonolysis, providing novel insight into the OH formation mechanism and applicability of the quantum chemical methods for studying such a reaction system.

(1) The calculated reaction and activation energies of the O_3–isoprene reactions are very sensitive to effects of electron correlation and basis set. The activation energies of primary ozonide formation were significantly underestimated with B3LYP/6-31G(d,p). The method using CCSD(T)/6-31G(d) + CF accurately predicted the activation energies of the primary ozonide formation. There are noticeable differences in the calculated reaction and activation energies for primary ozonide decomposition and carbonyl oxide unimolecular reactions between the methods of B3LYP/6-31G(d,p) and CCSD(T)/6-31G(d) + CF. We have demonstrated that the energetics predicted by CCSD(T)/6-31G(d) + CF agree well with those calculated by using high-level theories.

(2) The activation energies for the formation of the primary ozonides have been first determined. O_3 additions to the methyl-substituted and unsubstituted double bonds of isoprene were found to occur with comparable activation energies. Our results indicate that there is no significantly preferential branching for the initial step of the O_3–isoprene reactions. The calculated rate constant for the O_3–isoprene is in excellent agreement with the experimental value.

(3) Cleavage of the O_3–isoprene primary ozonides has been first investigated. The lowest barriers for the cleavage of **PO11** and **PO12** correspond to the paths to form syn (**CI2**) and anti (**CI4**) conformations, respectively. The difference in the activation energies between the syn and anti conformations, however, is relatively small (within 2.3 kcal mol^{-1} for **PO11** and 3.6 kcal mol^{-1} for **PO12**). Because of the large exothermicity associated with the formation of the primary ozonides, prompt dissociation of the excited primary ozonides leads to formation of syn and anti conformations each with a nonnegligible amount.

(4) Our study using high-level ab initio theory confirms the importance of carbonyl oxides on OH formation from the isoprene ozonolysis reported in a previous study.[16] OH formation occurs primarily via H-migration of the carbonyl oxides with the syn-positioned methyl (**CI2** or **CI6**).

(5) Last, this study presents thermochemical data and the potential energy surface of the O_3–isoprene reactions at a consistently high-level quantum chemical theory, and hence allows for elucidation of the mechanism of OH formation from ozonolysis of isoprene. We have determined an OH yield of 0.25 from prompt and thermal decomposition of the carbonyl oxides. Our calculated OH yield is in agreement with most experimental studies, further confirming our treatment of the OH formation mechanism.

Acknowledgment. This work was supported by the Robert A. Welch Foundation (Grant A-1417) and the Texas A&M University Supercomputing Facilities. We thank W. Lei for assistance with some calculations reported in this work and L. Thomson, Robert A. Duce, and Susan Solomon for helpful discussions. We also acknowledge the use of the Laboratory for Molecular Simulations at Texas A&M. Three reviewers provided valuable comments for improving this manuscript.

Supporting Information Available: Tables of absolute energies and zero-point energies and figures showing the structural parameters for all the species investigated in this study. This material is available free of charge via the Internet at http://pubs.acs.org.

JA011518L